Electrical Conductivity in Solid Solutions of $La_{5-x}M_xMo_3O_{16.5+x/2}$ (M = Ce^{4+} and Th^{4+}; $0.0 \leq x < 0.3$) with a Fluorite-Related Structure

M. Tsai and M. Greenblatt*

Department of Chemistry, Rutgers, The State University of New Jersey, Piscataway, New Jersey 08855

Received September 19, 1989

Solid solutions of $La_{5-x}M_xMo_3O_{16.5+x/2}$, where M = Ce^{4+} and Th^{4+} with $0.0 \leq x < 0.3$, with a fluorite-related structure have been prepared by solid-state reaction. The unit-cell parameters decrease with increasing Ce^{4+} content. Ionic conductivity was investigated from 200 to 700 °C by ac complex impedance measurement. The conductivity is enhanced for Ce^{4+} content up to $x \leq 0.25$. Conductivity due to electrons was not observed. The highest conductivity was found in $La_{4.95}Ce_{0.05}Mo_3O_{16.525}$, from $\sigma \sim 2.6 \times 10^{-6}$ $(\Omega\ cm)^{-1}$ with E_a = 66 eV at 200 °C to $\sigma \sim 8.0 \times 10^{-3}$ $(\Omega\ cm)^{-1}$ with E_a = 0.51 eV at 680 °C. Differential thermal analysis, thermogravimetry, and magnetic susceptibility measurements and X-ray absorption near-edge spectral analysis were also carried out. An interstitialcy mechanism is proposed to interpret the oxide ion conduction behavior in this type of oxygen-excess system.

Introduction

In compounds with a fluorite-type structure, high ionic conductivities are usually found due to the existence of vacancies and/or interstitial ions. The ionic conductivity can be enhanced by means of doping with aliovalent cations as, for example, in CaO- or Y_2O_3-stabilized zirconia,[1] where the O^{2-} ion conduction is via a vacancy mechanism, or as in $Ba_{1-x}U_xF_{2+2x}$ or $Pb_{1-x}U_xF_{2+2x}$,[2] where the F^- ion conduction is via an interstitial (interstitialcy) mechanism. Similar phenomena were also reported in the systems of $Pb_{1-x}Bi_xF_{2+x}$[3] and $Ca_{1-x}Y_xF_{2+x}$.[3,4]

In a recent study in our laboratory,[5] high oxide ion conductivities were found in a series of nonstoichiometric oxides, $Ln_5Mo_3O_{16.5}$ (Ln = La, Pr, Nd, Sm, and Gd). $La_5Mo_3O_{16.5}$ has the highest conductivity with $\sigma \sim 3 \times 10^{-3}$ $(\Omega\ cm)^{-1}$ and E_a = 0.84 eV at 680 °C.

$La_5Mo_3O_{16}$ and $La_5Mo_3O_{16.5}$ are isostructural with $CdY_4Mo_3O_{16}$ (space group $Pn3n$, Z = 4),[6,7] which has a structure closely related to that of CaF_2. The lattice parameters are a = 11.2238 (6) Å for the reduced phase, $La_5Mo_3O_{16}$, and a = 11.2400 (2) Å for the oxidized phase, $La_5Mo_3O_{16.5}$. The oxygen coordination polyhedra of the cations are shown at z = 0 (Figure 1a) and z = 0.25 (Figure 1b) in the unit cell. La atoms are located in 8 regular and 12 distorted eight coordination polyhedra; Mo atoms occupy 12 distorted tetrahedral sites for both reduced and oxidized phases. The O^{2-} sites are fully occupied in $La_5Mo_3O_{16}$ and in $La_5Mo_3O_{16.5}$ with two additional O^{2-} ions entering interstitial sites. These excess oxygens lead to an expanded unit cell in $La_5Mo_3O_{16.5}$ and contribute to the oxide ion conductivity.

To enhance the oxide ion conductivity and to further understand the conduction behavior of $Ln_5Mo_3O_{16.5}$, cations with formal oxidation state of 4+, Ce^{4+} and Th^{4+}, were partially substituted for La^{3+} to introduce more interstitial oxide ions. Similar studies have been made in anion-excess fluorides (e.g., $Ca_{1-x}Y_xF_{2+x}$[3,4]), where the relationship between structure and defect clusters has been investigated by various methods.[8-12] The enhanced ionic conductivity in anion-excess fluorite-type systems has been ascribed to the lowering of the activation energy due to the formation of defect clusters.[3,4]

In this paper we present the results of ionic conductivity studies in the substituted systems of $La_{5-x}M_xMo_3O_{16.5+x/2}$ (M = Ce^{4+}, Th^{4}) at 200–700 °C. In addition, the effect of Sr^{2+} substituted for La^{3+} in $La_{5-x}Sr_xMo_3O_{16.5-x/2}$ on the ionic conductivity was examined.

Experimental Section

All samples were prepared by solid-state reactions from appropriate amounts of the stoichiometric starting materials of CeO_2 (ThO_2), MoO_2, MoO_3, and La_2O_3, reagent grade or better, according to

$$(2x)CeO_2 + (5 - x)La_2O_3 + 5MoO_3 + MoO_2 \rightarrow 2La_{5-x}Ce_xMo^{VI}_2Mo^{V}O_{16+x/2}$$

The pelletized samples (pressed at 7000 lb) were sealed in evacuated silica ampules under 50–60 mTorr and fired at 960 °C for 3 days. Part of the product was oxidized in air for 1 day and in oxygen atmosphere for 2–3 days at 560 °C.

X-ray powder diffraction patterns were obtained on a Scintag Model PAD V unit with nickel-filtered copper radiation; the internal standard was molybdenum powder. Cell parameters were calculated by using a least-squares method.

Ionic conductivities were measured by an ac complex impedance technique using a Solartron Model 1250 frequency analyzer and 1186 electrochemical interface that were programmed by a Hewlett-Packard 9816 desktop computer for data collection and analysis. Contact to the samples was made by coating the faces of the pellets with platinum paste. The frequency range 10 Hz to 65 kHz was employed at a heating rate of 4 °C/min over the

* To whom the correspondence should be addressed.

(1) West, A. R. *Solid State Chemistry and Its Applications*; Wiley: New York, 1984; p 478.
(2) Ovwerkerk, M.; Schoonman, J. *Studies in Inorganic Chemistry*; Proceedings of the Second European Conference, Veldhoven, The Netherlands; Elsevier Scientific Publishing Company: Amsterdam, 1983; Vol. 3, p 247.
(3) Reau, J. M.; Lucat, C.; Campet, G.; Claverie, J. *Electrochim. Acta* **1977**, *22*, 761.
(4) Reau, J. M.; Lucat, C.; Campet, G.; Portier, J.; Hammou, A. *J. Solid State Chem.* **1976**, *17*, 123.
(5) Tsai, M.; Greenblatt, M.; McCarroll, W. H. *Chem. Mater.* **1989**, *1*, 253.
(6) Bourdet, J. B.; Chevalier, R.; Fournier, J. P.; Kohlmuller, R.; Omaly, J. *Acta Crystallogr.* **1982**, *B38*, 2371.
(7) McCarroll, W. H. *J. Solid State Chem.* **1983**, *48*, 189.
(8) Cheetham, A. K.; Fender, B. E. F.; Steele, D.; Taylor, R. I.; Willis, B. T. M. *Solid State Commun.* **1970**, *8*, 171.
(9) Catlow, C. R. A. *J. Phys. C* **1976**, *9*, 1845.
(10) Catlow, C. R. A. *J. Phys. C* **1976**, *9*, 1859.
(11) Cheetham, A. K.; Fender, B. E. F.; Cooper, M. J. *J. Phys. C.* **1971**, *4*, 3107.
(12) Steele, D.; Childs, P. E.; Fender, B. E. F. *J. Phys. C* **1972**, *5*, 2677.

0897-4756/90/2802-0133$02.50/0

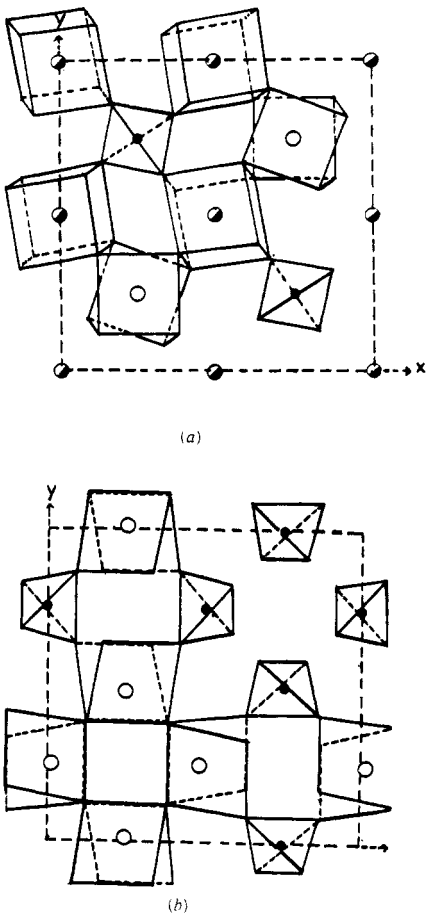

Figure 1. (a) Oxygen polyhedra for cations at $z = 0$, coordination number 8 La (◒) and coordination number 4 Mo (●); $z = 0.014$, distorted coordination number 8 La (○). (b) Oxygen polyhedra for cations (La, Mo) at $z = 0.25$.

temperature range 200–700 °C. All the measurements were carried out in air on the fully oxidized phases.

Thermogravimetry (TG) and differential thermal analysis (DTA) measurements were carried out on a Du Pont 9900 Model thermal analyzer. Magnetic susceptibility measurement were made on superconducting quantum interference device (SQUID, Quantum Design). The X-ray absorption near-edge spectrum (XANES) was recorded on the X-23 beam line at the National Synchrotron Light Source, Brookhaven National Laboratory.

Results and Discussion

The X-ray powder diffraction (XRD) of $La_{5-x}Ce_xMo_3O_{16.5+x/2}$ with $x \leq 0.3$ showed a single-phase pattern of the $La_5Mo_3O_{16}$ type.[5,7] For $x > 0.3$, CeO_2 is seen in the XRD as an impurity. The cell parameters decreased with increasing Ce^{4+} content (Figure 2). This is consistent with the smaller effective ionic radius of Ce^{4+} (1.11 Å) compared to that of La^{3+} (1.30 Å) in an 8-coordination site. It is noteworthy that the fully oxidized sample (curve 2, Figure 2), annealed in oxygen for 3 days, has a larger cell parameter than does the partially oxidized sample (curve 1, Figure 2), which was annealed in air for 1 day. The reason for such a rigorous condition required for complete oxidation of the $La_{5-x}Ce_xMo_3O_{16+x/2}$ phase is probably due to the large grain size of the samples. The larger grain size, compared to previously prepared $La_5Mo_3O_{16.5}$ samples,[5] is supported by sharper and more intense X-ray powder diffraction peaks, which is ascribed to the different sample preparative method (i.e., higher temperature and longer reaction time) required for the substitutional reactions in this study. This may also be the reason for the slightly lower conductivity of $La_5Mo_3O_{16.5}$ in this work compared

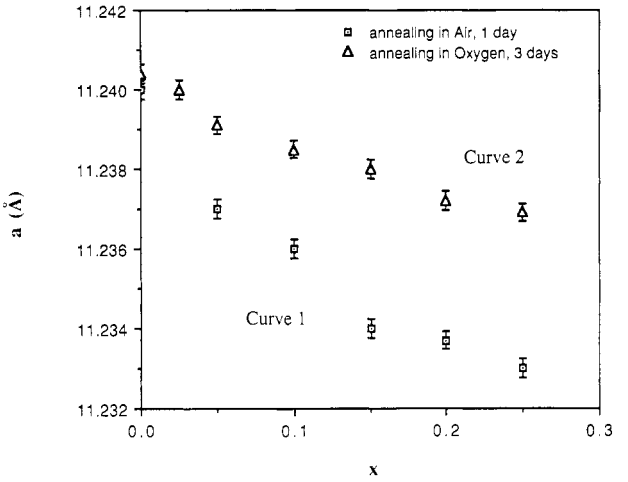

Figure 2. Cell parameter of $La_{5-x}Ce_xMo_3O_{16.5+(x/2)-y}$ as a function of Ce(IV) content, $0.0 \leq x \leq 0.3$; $y \sim 0$ for fully oxidized phases (annealing in oxygen, 3 days), $y > 0$ for partially oxidized phases (annealing in air, 1 day).

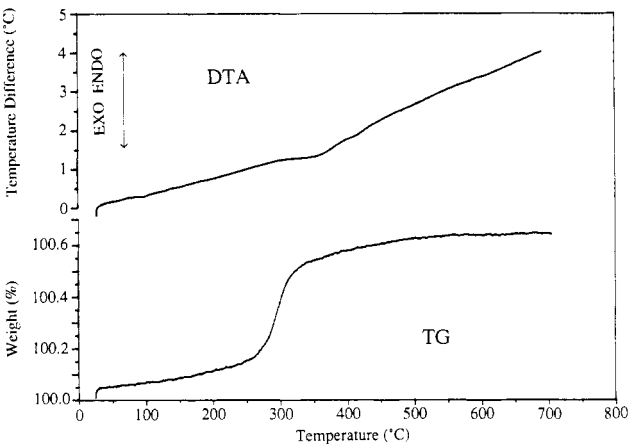

Figure 3. Differential thermoanalysis and thermogravimetry in the system of nominal composition $La_{4.95}Ce_{0.05}Mo_3O_{16.525}$; heating rate = 10 °C/min.

to previous results;[5] i.e., the higher concentration of defects associated with a smaller particle size material will enhance the ionic conductivity in the extrinsic region. For this reason, the $La_5Mo_3O_{16.5}$ sample studied here was also prepared by the same method that was used for the substituted samples.

In the DTA of "$La_{5-x}Ce_xMo_3O_{16+x/2}$" (Figure 3; i.e. the reduced phase), a broad exothermic peak at ~290 °C is due to reaction with oxygen. For "$La_{5-x}Ce_xMo_3O_{16+x/2}$" prepared under reducing conditions, charge compensation for the substituted Ce^{4+} may occur either by the uptake of $x/2$ oxygen as indicated in the formula or by reduction of Mo^{6+} in $La_{5-x}Ce_xMo^{5+}{}_{1+x}Mo^{6+}{}_{2-x}O_{16}$. The TG results (Figure 3) show that the oxygen uptake for all samples with different values of x in "$La_{5-x}Ce_xMo_3O_{16+x/2}$" is essentially 0.5. This is clear evidence that charge compensation for Ce^{4+} substitution in $La_{5-x}Ce_xMo_3O_{16+x/2}$ occurs by addition of $x/2$ interstitial oxygens. We have shown unambiguously that the fully oxidized phase of $La_5Mo^{5+}Mo^{6+}{}_2O_{16}$ leads to $La_5Mo_3O_{16.5}$ as expected.[5] If charge compensation for Ce^{4+} occurred by reduction of Mo^{6+}, we would expect the weight gain in the TG, due to oxygen uptake in $La_{5-x}Ce_xMo_3O_{16}$, to vary for different x values. Thus, in the fully oxidized substituted samples the total oxygen content is close to $16.5 + x/2$. This is also confirmed by magnetic susceptibility measurements which indicate diamagnetic properties for the fully oxidized samples.

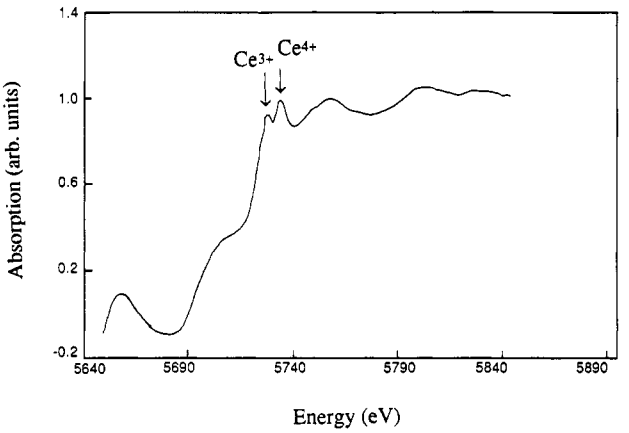

Figure 4. X-ray absorption near-edge spectrum of $La_{4.95}Ce_{0.05}Mo_3O_{16.525}$.

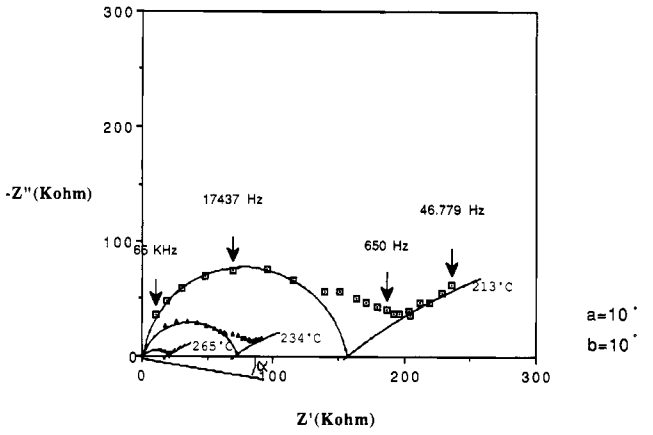

Figure 5. Ac complex impedance spectra at various temperatures in $La_{4.95}Ce_{0.05}Mo_3O_{16.525}$; where the semicircle intersects the Z' axis denotes the ohmic bulk resistance.

Moreover, the partially oxidized phases of the Ce^{4+}-substituted system show paramagnetic behavior, confirming the presence of some Mo^{5+}. These results are consistent with the impedance data (to be discussed) that show the absence of electronic conductivity due to mixed-valent Mo^{5+}/Mo^{6+} (i.e., the semicircles intersect Z'' vs Z' at x and $y = 0.0$; see Figure 5).

X-ray absorption near edge spectroscopy (XANES) was carried out to determine the formal oxidation state of the Ce ion in the oxidized phases (Figure 4). The data, similar to those of CeO_2,[13,14] were fitted to obtain an oxidation state of ~3.7+ for Ce in $La_{5-x}Ce_xMo_3O_{16.5+x/2}$. This may indicate the possible existence of mixed-valent Ce^{3+}/Ce^{4+}. However, the magnetic susceptibility measurements indicate that the fully oxidized samples are diamagnetic at room temperature. Moreover, the sample is pale yellow.

Typical ac complex impedance spectra at various temperatures are shown in Figure 5. The bulk (electrolyte) and the electrode–electrolyte effects are evident by the presence of two semicircles at lower temperature (200–300 °C) or a semicircle and a straight line at higher temperature (>300 °C). The semicircle is depressed by an angle of 10°. This may be due to the surface imperfection associated with current inhomogeneities or the relaxation time distribution.[15] Figure 6 shows the Arrhenius plots

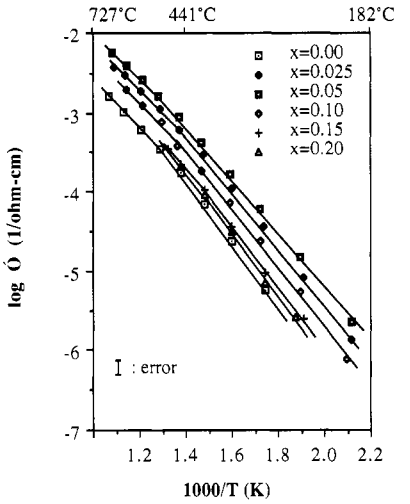

Figure 6. Arrhenius plot of conductivity in $La_{5-x}Ce_xMo_3O_{16.5+x/2}$ in the temperature range 200–680 °C.

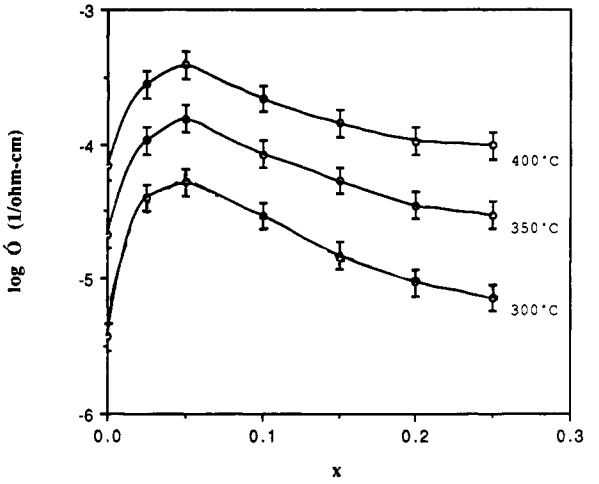

Figure 7. Isotherms of the conductivity in $La_{5-x}Ce_xMo_3O_{16.5+x/2}$.

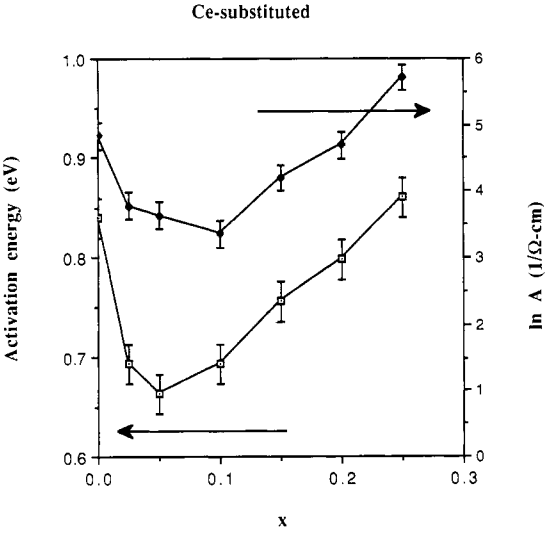

Figure 8. Activation energy (E_a) and preexponential factor (A) vs x in $La_{5-x}Ce_xMo_3O_{16.5+x/2}$. The data were determined by the least-squares method at 300–450 °C.

of the bulk conductivity of $La_{5-x}Ce_xMo_3O_{16.5+x/2}$. A change in the slope of log σ vs $1/T$ was observed for all the samples at high temperature (>550 °C). This is attributed to the existence of a long-range type of Debye–Hückel attractive force between defects of opposite charge, e.g., between vacancies and interstitials.[16] Figure 7 represents the

(13) Kotani, A.; Mizuta, H.; Jo, T.; Parlebas, J. C. *Solid State Commun.* **1985**, *53*, 805.
(14) Jo, T.; Kotani, A. *Solid State Commun.* **1985**, *54*, 451.
(15) (a) Vischjager, D. J.; Van Der Put, P. J.; Schram, J.; Schoonman, J. *Solid State Ionics* **1988**, *27*, 199. (b) Macdonald, J. R. *Impedance Spectroscopy*; Wiley: New York, 1987; p 16.

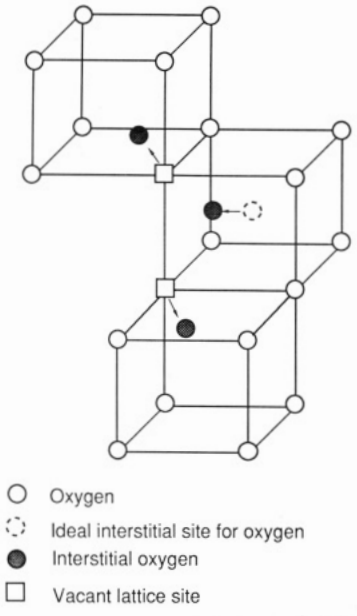

Figure 9. Ideal interstitial defect cluster in UO_{2+x}. Uranium positions (not shown) are located in the center of every other cube.

conductivity isotherms of $La_{5-x}Ce_xMo_3O_{16.5+x/2}$ at 300, 350, and 400 °C as a function of x. The conductivity increases for $x \leq 0.05$ and then decreases with increasing x. The change in conductivity with increasing x is significantly larger in the low-temperature region. This may have important applications for using this material as an oxygen sensor at moderate temperature. Figure 8 shows the variations of activation energy (E_a) and preexponential factor (A) as a function of x (i.e., E_a and A are defined by the Arrhenius equation $\sigma = Ae^{-E_a/RT}$).

A comparison of Figures 7 and 8 suggests that the conductivity is more strongly affected by the activation energy (E_a) than by the preexponential factor (A) in the low-dopant regime ($x \leq 0.05$). The conductivity increases due to the dramatic decrease of E_a (Figure 8), which may be ascribed to the creation of an easier path for the oxide ions to migrate through the lattice, for example, by formation of defect clusters. On the other hand, the decrease of A may be due to a decrease in entropy. A is proportional to the carrier concentration (N), which is also an exponential function of entropy change and activation energy for the creation of mobile ions, i.e., $N = N_0 \times \exp(\Delta S_f/R) \times \exp(-E_f/RT)$. Here, E_f has been included in E_a ($=E_m + E_f$, migration and formation energy), so only ΔS has to be considered. According to theories of ionic diffusion in solids, defects involving interstitial atoms will lead to $\Delta S < 0$.[17] Thus increasing the interstitial population will decrease the entropy and hence the exponential factor A. This phenomenon will be more pronounced if the interstitial atoms are associated in defect clusters.

For $x > 0.05$, both E_a and A increase slowly with increasing Ce^{4+} content, and this results in a net decrease in the conductivity until at $x = 0.25$ the conductivity is equal to that of $La_5Mo_3O_{16.5}$. This may be due to the progressive loss of vacancies, which are gradually occupied by the inserted oxide ions. This may explain the constancy of the lattice parameter in this composition range ($0.10 \leq x \leq 0.25$); i.e., the electrostatic repulsion between the inserted and lattice oxide ions counteract the decrease in the

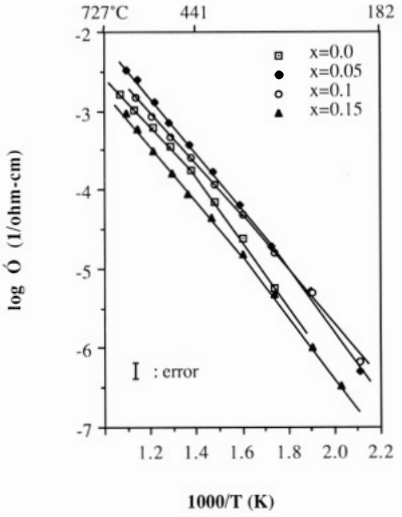

Figure 10. Arrhenius plot of conductivity in $La_{5-x}Th_xMo_3O_{16.5+x/2}$ in the temperature range 200–680 °C.

cell parameter that might result from the smaller Ce^{4+} replacing the La^{3+} ion. This phenomenon also suggests that the conduction is by an interstitialcy mechanism. Alternatively, the constancy of the lattice parameters for $x > 0.1$ may indicate the limit of solid-solution formation.

Models of defect clusters may be helpful for interpreting the conduction behavior. For example, in the case of UO_{2+x} in place of a single interstitial atom, the cluster appears to contain three interstitial oxygens and two vacancies (Figure 9).[18-20] Thus, for small values of x, in addition to having interstitial ions, vacancies must also be created. The latter contribute to the lowering of activation energy, since oxide ions migrate via interstitialcy mechanism. A similar interpretation may be applied to the $La_{5-x}Ce_xMo_3O_{16.5+x/2}$ system, although there is no information about the nature of defect clusters in this system (i.e., by neutron diffraction).

Moreover, in $Pb_{1-x}Bi_xF_{2+x}$[3] the decrease of E_a for low values of x was ascribed to the formation of defect clusters similar to those found in UO_{2+x}, and an interstitialcy mechanism of ionic motion was proposed to explain the fluoride ion conductivity. Because of the similarity in the conduction behavior of $La_{5-x}Ce_xMo_3O_{16.5+x/2}$ and $Pb_{1-x}Bi_xF_{2+x}$, it is proposed that the ionic conduction in $La_{5-x}Ce_xMo_3O_{16.5+x/2}$ is dominated by an interstitialcy mechanism.

Thorium substitution in $La_5Mo_3O_{16.5}$ was undertaken to confirm that the enhanced conductivity observed in the Ce^{4+}-substituted samples is essentially due to the excess interstitial oxide ions (i.e., $x/2$ oxide ions in $La_{5-x}Ce_xMo_3O_{16.5+x/2}$) and not due to electrons resulting from the Ce^{3+}/Ce^{4+} mixed valency. Qualitative two-probe dc measurements on this sample confirm an absence of conductivity due to electrons. The conductivity behavior of $La_{5-x}Th_xMo_3O_{16.5+x/2}$ (Figures 10 and 11) is similar to that of $La_{5-x}Ce_xMo_3O_{16.5+x/2}$.

In contrast, no change in conductivity or activation energy was found between $La_5Mo_3O_{16.5}$ and Ce^{3+}-substituted $La_{5-x}Ce_xMo_3O_{16.5}$ for $0.025 \leq x \leq 0.15$. This is because the effective ionic radii of Ce^{3+} and La^{3+} are similar; thus the size of the "bottleneck" for ionic motion is not affected.

(16) West, A. R. *Solid State Chemistry and Its Applications*; Wiley: New York, 1984; p 326.
(17) Shewmon, P. G. *Diffusion in Solids*; J. Williams Book Co.: Jenks, OK, 1983; p 67.
(18) West, A. R. *Solid State Chemistry and Its Applications*; Wiley: New York, 1984; p 331.
(19) Lynds, L.; Young, W. A.; Mohl, J. S.; Libowitz, G. G. Nonstoichiometric Compounds. *Adv. Chem. Ser., No. 39*, **1963**, 58.
(20) Willis, B. T. M. Nonstoichiometric Compounds. *Adv. Ceram.* **1986**, *23*, 711.

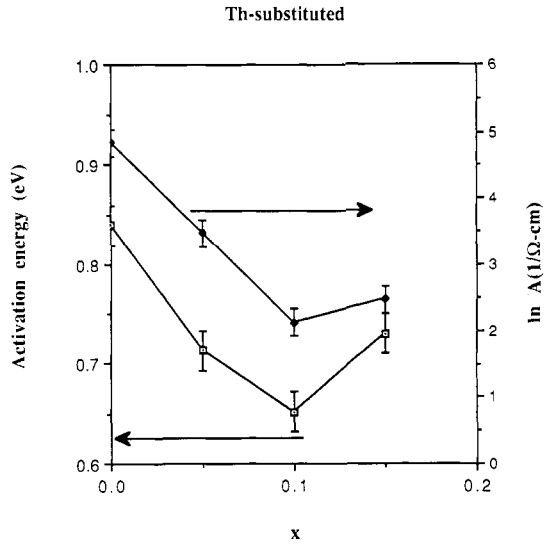

Figure 11. Activation energy (E_a) and preexponential factor (A) vs x in $La_{5-x}Th_xMo_3O_{16.5+x/2}$. The data were determined by the least-squares method at 300–450 °C.

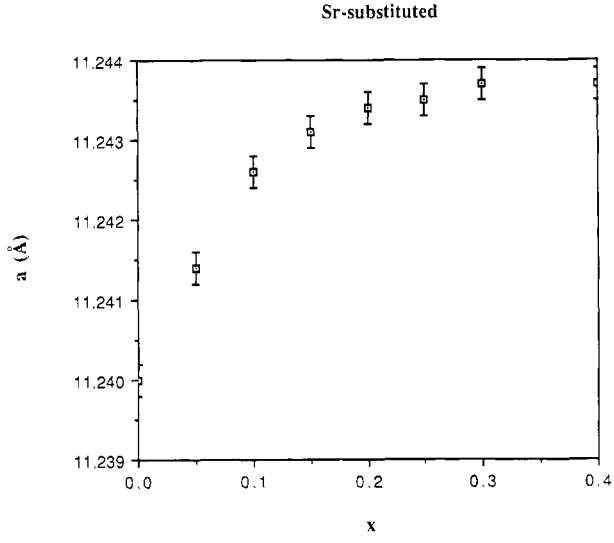

Figure 12. Cell parameter of $La_{5-x}Sr_xMo_3O_{16.5-x/2}$ as a function of Sr^{2+} content, $0.0 \leq x \leq 0.30$.

In $La_{5-x}Sr_xMo_3O_{16.5-x/2}$ ($0.05 \leq x \leq 0.20$) the cell parameters increased with increasing Sr^{2+} content (Figure 12), due to the larger effective ionic radius (1.40 Å) of Sr^{2+}, compared to that of La^{3+} (1.30 Å) in a 8 coordination site. No apparent change in conductivity or activation energy was observed, as compared to $La_5Mo_3O_{16.5}$. This can be attributed to two opposing effects: the decrease in the concentration of mobile oxide ions (i.e., $x/2$ less than in $La_5Mo_3O_{16.5}$) tends to decrease the conductivity, while the larger "bottleneck" for ionic motion would tend to increase the conductivity. A slight decrease of the preexponential factor may be noticed in Figure 13.

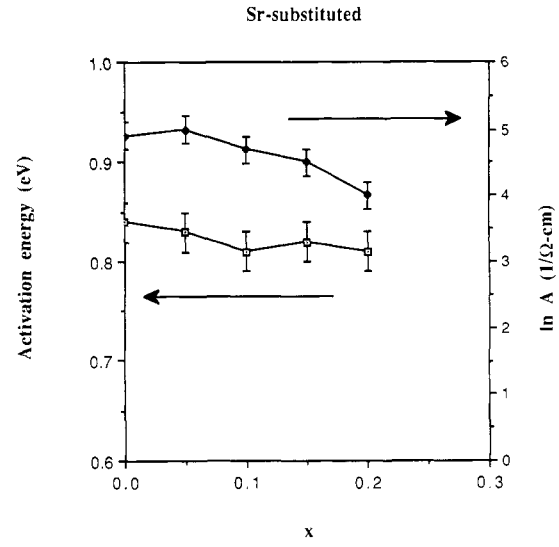

Figure 13. Activation energy (E_a) and preexponential factor (A) vs x in $La_{5-x}Sr_xMo_3O_{16.5-x/2}$. The data were determined by the least-squares method at 300–450 °C.

Conclusion

The oxide ion conductivity of $La_5Mo_3O_{16.5}$ can be enhanced by substituting small amounts of La^{3+} by Ce^{4+} or Th^{4+}, which was shown to increase the concentration of interstitial oxygen ions. The highest conductivity was found in $La_{4.95}Ce_{0.05}Mo_3O_{16.525}$: $\sigma \sim 2.6 \times 10^{-6}$ $(\Omega\ cm)^{-1}$ and $E_a = 0.66$ eV at 200 °C; $\sigma \sim 8 \times 10^{-3}$ $(\Omega\ cm)^{-1}$ and $E_a = 0.51$ eV at 680 °C. The interstitialcy mechanism is proposed to interpret the oxide ion conduction behavior in this oxygen-excess compound with fluorite-related structure. No apparent change in conductivity or E_a but a slight decrease in A was found for $La_{5-x}Sr_xMo_3O_{16.5-x/2}$ ($0.05 \leq x \leq 0.20$).

Acknowledgment. We gratefully acknowledge G. Liang for the XANES data and Dr. W. H. McCarroll, Dr. S. Tanase, and Shu Li for helpful discussions. This research was supported by the office of Naval Research.

Registry No. $La_5Mo_3O_{16.5}$, 119454-70-5; $Ce_{0.02}La_{4.98}Mo_3O_{16.51}$, 124890-39-7; $Ce_{0.05}La_{4.95}Mo_3O_{16.52}$, 124890-40-0; $Ce_{0.1}La_{4.9}Mo_3O_{16.55}$, 124890-41-1; $Ce_{0.15}La_{4.85}Mo_3O_{16.58}$, 124890-42-2; $Ce_{0.2}La_{4.8}Mo_3O_{16.6}$, 124890-43-3; $Th_{0.05}La_{4.95}Mo_3O_{16.52}$, 124890-44-4; $Th_{0.1}La_{4.9}Mo_3O_{16.55}$, 124890-45-5; $Th_{0.15}La_{4.85}Mo_3O_{16.58}$, 124890-46-6; $La_{4.7-5}Sr_{0-0.3}Mo_3O_{16.35-16.5}$, 124890-47-7.